SUBSTRATE DEPENDENCE OF CsK$_2$Sb PHOTO-CATHODES PERFORMANCE

L. Guo[1*], M. Kuriki[1],

Graduate School for Advanced Sciences of Matters, Hiroshima University,
Higashihiroshima, Hiroshima 739-8530, Japan

K. Negishi[2]

Iwate University, 3-18-8 Ueda, Morioka, Iwate 020-8550, Japan

Abstract

A photo-cathode which is able to generate a high-performance electron beam with large operability is one of the most important devices in the advanced accelerator. In particular, the CsK$_2$Sb photo-cathode is paid attention because it has high robustness and can be driven by visible light. In this study, we performed cathode evaporation on Si(100), Si(111), and GaAs(100) substrates to evaluate the performance dependence on the substrate material and surface state. For each substrate, the cathode performances on the as-received and cleaned substrates were compared. We found that the cathode performance on the cleaned substrate was superior to that on the as-received substrate for all materials. The cathode performances on the cleaned GaAs(100) and Si(100) substrates were similar, but it on the cleaned Si(111) was significantly much lower. This result gave an experimental evidence about substrate surface direction dependence of CsK$_2$Sb photo-cathode performance.

INTRODUCTION

In linear-accelerator-based advanced accelerators such as the Energy Recovery Linac (ERL) [1] [2] and Free Electron Laser (FEL) [3], the performance of the accelerated beam strongly depends on the initial beam property. Therefore, the beam performance from the source is important. For example, a high brightness electron beam with more than 10 mA average current and less than 1.0 πmm·mrad [4] emittance is required for the next generation ERL-based synchrotron radiation (SR) facility [1]. Since 1980, a photo-cathode has been operated as an advanced electron source in many accelerators [5].

Multi-alkalis are a group of materials composed from two or more alkali metals. Multi-alkali materials have been used as photo-cathodes in photo-multiplier tubes [6]. The multi-alkali cathode is considered to be the strongest candidate as a high brightness electron source because it can be operated by green light (532 nm) with 10% QE [7] [8], which is easily obtained from the second harmonics of a solid-state laser. Moreover, the multi-alkali cathode has a long operational lifetime [9].

CsK$_2$Sb cathode is fabricated as a thin film on a substrate by evaporation in an ultra-high vacuum environment. Various materials have been examined as the substrate, e.g. Glass(amorphous) [10], Cu(amorphous) [11] [12], SUS [12] [13] [14], Mo(amorphous) [12] [14], Mo(100) [7], Si(100) [8], GaAs(100) [15], where the numbers in parenthesis are the surface direction of the crystalline substrate.

Cs$_3$Sb cathode has proven to depend strongly on the chemistry of substrate surface [16]. XPS studies for the CsK$_2$Sb cathode [14] [17] suggest that the cathode performance strongly depends on the substrate surface state (oxidation, etc.).

Cathodes fabricated on the amorphous substrates (Glass, Cu, SUS, and Mo) showed relatively low QE as 1-5% with 532nm laser light [10] [11] [12] [13] [14]. In contrast, cathodes fabricated on crystalline substrates (Si(100), Mo(100) and GaAs(100)) showed relatively high QE as 7-10% with 532nm laser light [7] [8] [15]. These results suggest that the substrate crystallinity has an impact on the cathode performance.

CsK$_2$Sb crystal direction was studied with XRD [18] [19]. The quantum efficiency of the cathode in these studies was relatively low (3 %) and the cathode performance dependence on the surface direction of the substrate or CsK$_2$Sb crystal was not significantly observed. It suggests that the cathode evaporation condition was not fully optimized in these studies.

By comparing the cathode evaporated with an optimized condition, on substrates in different surface directions, we expect to reveal the dominant factor for the cathode performance, whether cleanness, crystallinity, or surface direction of the substrate.

For that purpose, CsK$_2$Sb cathode was fabricated on Si(100), Si(111), and GaAs(100) and the performance was compared. To observe the dependence significantly, the cathode evaporation condtion was optimized at first. For each substrate, the as-received and cleaned surfaces were examined. In the next sections, we describe the experiment, and provide the results and discussion.

EXPERIMENT

The experimental setup was described in Ref. [20]. The cathode was fabricated in a vacuum chamber at a typical pressure of 1.0×10^{-8} Pa. The cathode substrate is fixed on a molybdenum puck. The puck is mounted on the cathode holder during evaporation and electron emission. In this study, Si(100) and Si(111) p-type wafers with a resistivity of ≤ 0.002 Ωcm^{-1} and GaAs(100) p-type wafers are employed as the substrates.

---

* d120366@hiroshima-u.ac.jp

The Si(100) and Si(111) substrates were processed with a 5% HF solution for about 5 min to remove the surface oxidized layer [21]. The GaAs surface was processed with a H_2SO_4:H_2O_2:H_2O (4:1:1) solution for about 5 min to remove the surface oxidized layer [22].

To examine the effect of the surface oxidation, we also examined the as-received substrates [23] [24]. The atomic arrangement of the as-received surface is disturbed by the oxidation layer [25], and it is considered to be amorphous [24] [25].

The evaporation sources are mounted on a linear movement mechanism in the chamber. The high-purity (99.9999%) Sb pellets were resistively heated in a tungsten evaporation basket. The K and Cs sources are dispensers provided by SAES Getters Co., Ltd. [26]. The amount of material on the substrate was monitored with a quartz thickness monitor (INFICON Q-pod Quartz Crystal Monitor). The thickness monitor is placed in a symmetrical position to the cathode substrate in order to absorb an equivalent amount of vapor. The source to substrate distance was maintained at about 12 mm during the evaporation.

To control the cathode temperature, a tungsten heater is used. The heater is mounted on the head of the linear mover, which can be inserted from back side of the cathode puck. The cathode puck temperature is measured with a thermocouple.

Typically the CsK_2Sb cathode was formed by sequential evaporation of Sb, K, and Cs on a substrate. 10 nm Sb was evaporated at 100°C substrate temperature giving maximum QE with less fluctuation [20]. Amount of K and Cs were automatically determined giving the maximum QE after each evaporation, i.e. we stopped the evaporation whenever QE is saturated. The evaporation procedure is explained in Ref. [20].

QE was measured with a 532 nm laser. The cathode was biased at -100 V, and the photo-current was measured as the current of the bias supplier. We examined Si(100), Si(111), and GaAs(100) substrates. The results (maximum QE) are summarized in Table 1 including the results of the preceding studies. We repeated the evaporation five times for each substrate. After each evaporation, the substrate was heated to initialize the surface. The error is obtained as the standard deviation of the five measurements, and it is statistical only. The QE of the as-received substrate was around 2.5-5.5% at 532 nm. The cleaned Si (100) and GaAs(100) substrates showed a good QE as high as 10%. These results are similar to those of the cleaned Mo(100) [7] and Si(100) substrates obtained by the Cornell group [8]. In contrast, the QE of the cleaned Si(111) was higher than that of the as-received Si(111), but it is much lower than that of the cleaned Si(100) and GaAs(100) substrates.

According to results shown in Table 1, the cathode performance developed on the cleaned substrate was significantly higher than that on the as-received substrate for all cases. We could not conclude that the substrate crystallinity has an impact on the cathode performance, because the chemical property of the oxidized surface may differ from the clean

Table 1: The maximum QE of the CsK_2Sb photo-cathode on Mo(100), Mo(amorphous), Si(100), Si (111), and GaAs (100) substrates at 532 nm are summarized.

Substrate	Surface treatment	QE[%]@532nm
Mo(100)	Polished+sputter	10.0 [7]
Mo(amorphous)	Polished+sputter	2-5 [12] [14]
Si(100)	as-received	4.8 ± 0.6
Si(100)	5%HF	9.4 ± 0.7
Si(100)	5%HF	$7 - 10$ [8]
Si(111)	as-received	1.6 ± 0.1
Si(111)	5%HF	2.3 ± 0.3
GaAs(100)	as-received	5.5 ± 0.2
GaAs(100)	H_2SO_4:H_2O_2:H_2O	10.0 ± 0.2

one, but it can be a collateral evidence. The cathode formed on the Si(111) substrate showed the least performance in the tested substrates in both the cleaned and as-received cases. The difference in the cathode performance on the Si(100) and Si(111) substrates provide direct evidence that the cathode performance depends strongly on the substrate direction, because the material properties of Si(100) and Si(111) are exactly same otherwise. A similar conclusion was also obtained by comparing QE of the crystalline Mo(100) [7] and amorphous Mo [12] [14], because the physical property of the crystalline and amorphous Mo other than the surface atomic arrangements, are almost same. Mo(100) and Mo(amorphous) substrates in Reference [7] [12] [14] are considered to be cleaned because it was polished and sputtered.

By considering these facts, the cathode performance depends not only on cleanness and crystallinity, but also on surface direction of the crystalline substrate. This is the first experimental evidence that CsK_2Sb cathode performance depends on the crystal surface direction of the substrate.

In the following section, we discuss these results.

DISCUSSION

Crystalline CsK_2Sb forms a DO_3 cubic structure [27] [28]. The unit cell contains four formula units and is represented by four face-centered sub-lattices shifted by $a\sqrt{3}/4$ (a is a lattice constant of the primitive translation vector) along the body diagonal [27] [29]. The lattice constant a is 8.61 [27] [28] [30].

Figure 1 and Figure 2 shows that the surface atomic arrangements of CsK_2Sb(100), CsK_2Sb(111), Mo(100), GaAs(100), Si(100), and Si(111) surfaces. By considering the matching between the atomic arrangements among CsK_2Sb (100), (111), Si(100), Mo(100), and GaAs(100) surfaces, CsK_2Sb are grown in (100) direction on Si(100), Mo(100), and GaAs(100) surfaces, and in (111) direction on Si(111) direction.

The reason for the reduced performance of the as-received substrates comparing to the cleaned substrates could be the less quality of CsK_2Sb crystal. Oxidation distorts the atomic
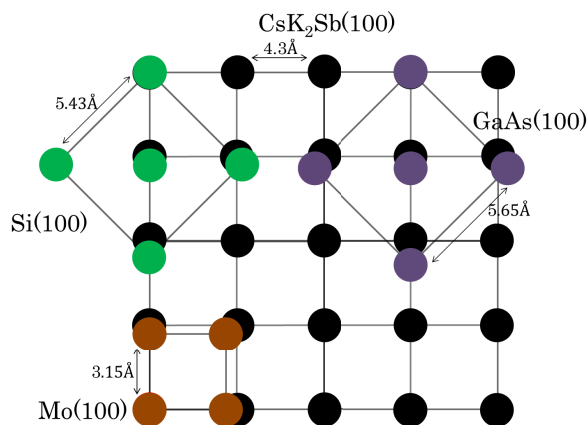
Figure 1: Atomic arrangement of CsK$_2$Sb(100) on the Mo(100), GaAs(100) and Si(100) surfaces. The lattice constants of Mo, Si, and GaAs are 3.15Å, 5.43Å, and 5.65Å, respectively [31].
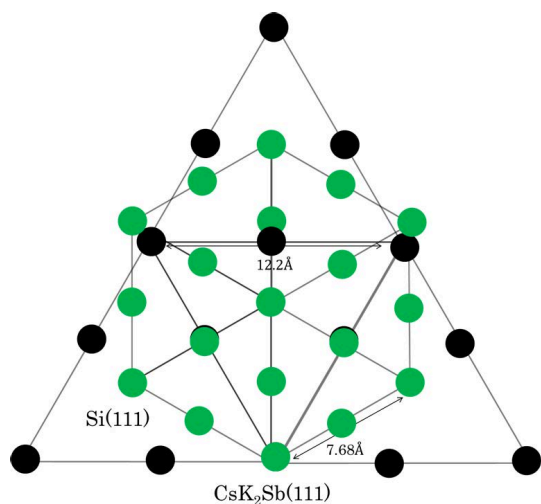

Figure 2: Atomic arrangement of CsK$_2$Sb(111) on the Si(111) surface.

arrangement of the substrate surface resulting a poor matching between the substrate and CsK$_2$Sb crystals. The poor matching leads to a lower quality of CsK$_2$Sb crystal grown on the substrate and reduced performance.

The cathode on the cleaned Si (100) and GaAs(100) substrates showed a good QE as high as 10%. These results are similar to those on the cleaned Mo(100) and Si(100) substrates obtained by the Cornell group [7]. On the other hand, the cathode performance on Si (111) is less than the others. These results can be explained with the band structure of CsK$_2$Sb. In References [27] [28], the bulk band dispersion of CsK$_2$Sb was calculated. The point on the boundary surface of the Brillouin region is called the K, L, and X points in the (110), (111), and (100) directions, respectively. According to the bulk band dispersion, CsK$_2$Sb is a direct transition type at the Γ point with 1.1 eV bandgap. The

bandgap is about 2.1, 3.1, and 1.4eV at K, L, and X, respectively. If we consider the photo-electron emission in (100) direction, not only electrons at Γ point, but also electrons at X point contributes to the emission, because the bandgap at X point is similar to that at Γ. On the other hand, for the photo-electron emission in (111) direction, there is no contribution at L point, because the bandgap energy (3.1 eV) is larger than the laser photon energy (2.3 eV at 532 nm). The photo-electron emission of CsK$_2$Sb in (111) direction is possible only at Γ point and this is the reason why the quantum efficiency of (111) surface is less than that of (100) surface.

By a similar consideration, the QE of (110) surface should be less than that of (100) surface. In the preceding studies [18] [19], CsK$_2$Sb was grown in (200) or (220) directions on Si (100) substrate, depending on the case and the cathode performance of (200) and (220) were similar [18]. We consider that the cathode evaporation conditions in these experiments were not fully optimized, because the QE is only 3% for 532 nm light in both cases. That is why CsK$_2$Sb crystal direction depends on the case and there was no significant difference on the cathode performance grown in (100) and (110) directions in these studies.

In our case, the cathode evaporation condition was carefully optimized and the cathode performance reproducibility was quite good. The cathode performance dependence on the substrate crystallinity and the surface direction was confirmed based on the reliable experiments.

SUMMARY

We studied the substrate dependence of CsK$_2$Sb photo-cathode performance. We studied GaAs(100), Si(100), and Si(111) as the substrates, and found that the cleaned substrates resulted in higher performance than the as-received substrates for all materials. By comparing cathodes on GaAs(100), Si(100), Si(111), and Mo [7] [12] [14], we found that the cathode on GaAs(100), Si(100), and Mo(100) had significantly better performance than that on Si(111) and Mo(amorphous). It showed that the cathode performance depends strongly not only the substrate material and surface state, but also the crystallinity and the surface direction. We obtained the first experimental evidence about substrate surface direction dependence of CsK$_2$Sb photo-cathodes performance. This fact has an impact on the accelerator sciences, because there is some potential to improve thin-film cathode performance by revisiting the substrate crystallinity and surface direction.

REFERENCES

[1] ERL Conceptual Design Report, KEK Report 2012-4 (2012).

[2] Georg H. Hoffstaetter *et al.*, Cornell Energy Recovery Linac Science Case and Project Defnition Design Report, Cornell University (2013.6).

[3] M. Altarelli *et al.*, The European X-ray Free Electron Laser Technica Design Report, DESY 2006-97 (2006).

[4] Sol M. Gruner *et al.*, Rev. Sci. Instrum. **73**, 1402 (2002).

[5] E. Chevallay *et al.*, Nucl. Instrum. Methods Phys. A**340**, 146 (1994).

[6] `https://www.hamamatsu.com/resources/pdf/etd/PMT_TPMZ0002E.pdf`

[7] M. A. Nichols, Research Experiences for Undergraduates (REU) Report, 2011, Cornell University. (available at: www.lepp.cornell.edu/ ib38/reu/11/Nichols_report.pdf (2011)].

[8] S. Karkare *et al.*, Proceedings of IPAC 2013, Pasadena, CA, TUOAB1 (2013).

[9] L. Cultrera *et al.*, Proceedings of 2011 Particle Accelerator Conference, New York, NY, WEP244 (2011).

[10] A. V. Lyashenko *et al.*, Journal of Instrumentation, Volume **4**, (July 2009).

[11] J. Smedley *et al.*, AIP Conf. Proc. **1149**, 18th Int'l. Spin Physics Symp., pp.1062-1066(2009).

[12] A. Burrill *et al.*, 21st IEEE Particle Accelerator Conference, Knoxville, TN, USA, 16 - 20 May 2005, pp.2672.

[13] M. Kuriki *et al.*, Proceedings of IPAC2016, Busan, Korea (2016).

[14] Valeri. S *et al.*, 4th European Particle Accelerator Conference, London, UK, 27 Jun-1 Jul 1994, pp.1459.

[15] M. A. A. Mamun *et al.*, J. Vac. Sci. Technol. A **34**, 021509 (2016).

[16] A.H. Sommer, Photoemissive Materials: Preparation, Properties and Uses (1968).

[17] S. Schubert *et al.*, Proceedings of IPAC2013, Shanghai, China, MOPFI005 (2013).

[18] M. Ruiz-Oses *et al.*, APL Materials **2**, 121101 (2014)

[19] S. Schubert *et al.*, Journal of Applied Physics **120**, 035303 (2016).

[20] L. Guo *et al.*, PTEP, 2017, 033G01.

[21] Karen Reinhardt and Werner Kern, Handbook of Silicon Wafer Cleaning Technology 9.2.2 William Andrew; 2 edition (2008/1/24).

[22] O. E Tereshchenko *et al.*, Appl. Surf. Sci. **142**, 75 (1999).

[23] W. Shin, H. Cho *et al.*, Phys. Soc. **54**, 1077 (2009).

[24] C. Logofatu *et al.*, in *Crystalline Silicon - Properties and Uses*, (InTech, 2011) Chap. 2.

[25] K. Kutsuki *et al.*, Sci. Tech. Adv. Mater. **8**, 204 (2007).

[26] `https://www.saesgetters.com/sites/default/files/AMD%20Brochure_0.pdf`

[27] L. Kalarasse *et al.*, J. Phys. Chem. Solids **71**, 314 (2010).

[28] A. R. H. F. Ettema *et al.*, Phys. Rev. B **66**, 115102 (2002).

[29] R. W. G. Wyckoff, *Crystal Structures* (Wiley, New York, 1960), Vol. 2.

[30] W. H. McCarroll, J. Phys. Chem. Solids **26**, 191 (1965).

[31] C. Kittel, *Introduction to Solid State Physics* (Wiley, 2004), 8th ed.